

Introduction

The European Space Agency's Herschel Space Observatory [1], launched on the 14th of May 2009, is designed to provide unfettered access to the far-infrared spectral region by means of three instruments. One of the instruments is the Spectral and Photometric Imaging Receiver (SPIRE) [2] which employs a Fourier transform spectrometer with feed-horn coupled bolometers to provide imaging spectroscopy.

The wavelength dependent beam of the individual feed-horns is complex, which makes the interpretation of the resulting spectral images challenging. We present a series of observations and the analysis conducted to determine the wavelength dependence of the SPIRE spectrometer beam profile.

Observations and data reduction

The wavelength dependent beam profile for the SPIRE FTS was determined by obtaining a spectrum at each spatial position as Neptune and Uranus were independently scanned across the field of view of the spectrometer.

Neptune and Uranus were used because they are both good approximations of point sources and are both bright in the infrared, which leads to a high signal-to-noise ratio in measurements.

Table 1: Observation details of the data used in our analysis.

Source	OD	Res	Reps	Raster grid	Step (")
Neptune	210	MR	2	90"x90"	9
	742	LR	6	84"x84"	7
Uranus	410	MR	2	70"x70"	7
	767	HR	4	Cross (90")	7.5
	767	HR	4	Cross (90")	7.5

[OD: Operational Day from the launch of the telescope, Res: Spectral Resolution, LR: Low resolution, MR: Medium resolution, HR: High resolution, Reps: Number of repetitions.]

The primary Neptune observation on Herschel operational day 210 consisted of medium spectral resolution ($\Delta\sigma = 0.24 \text{ cm}^{-1}$) FTS scans with two repetitions (i.e. 4 interferograms) per raster position.

The relative signal values and their errors were calculated using the Herschel Interactive Processing Environment (HIPE) data pipeline version 7 [4].

The data were produced in the form of a 3-D cube with two angular coordinates (RA and Dec) and one spectral coordinate, resulting in a complete SPIRE FTS spectrum at each of the points on the 11x11 (90"x90") raster grid.

The raster grid, initially in the equatorial coordinate system, is aligned with the spacecraft coordinate frame through a rotation matrix determined from the orientation of the spacecraft at the time of observation [3]. The other observations used in this analysis are described in Makiwa et al. [5].

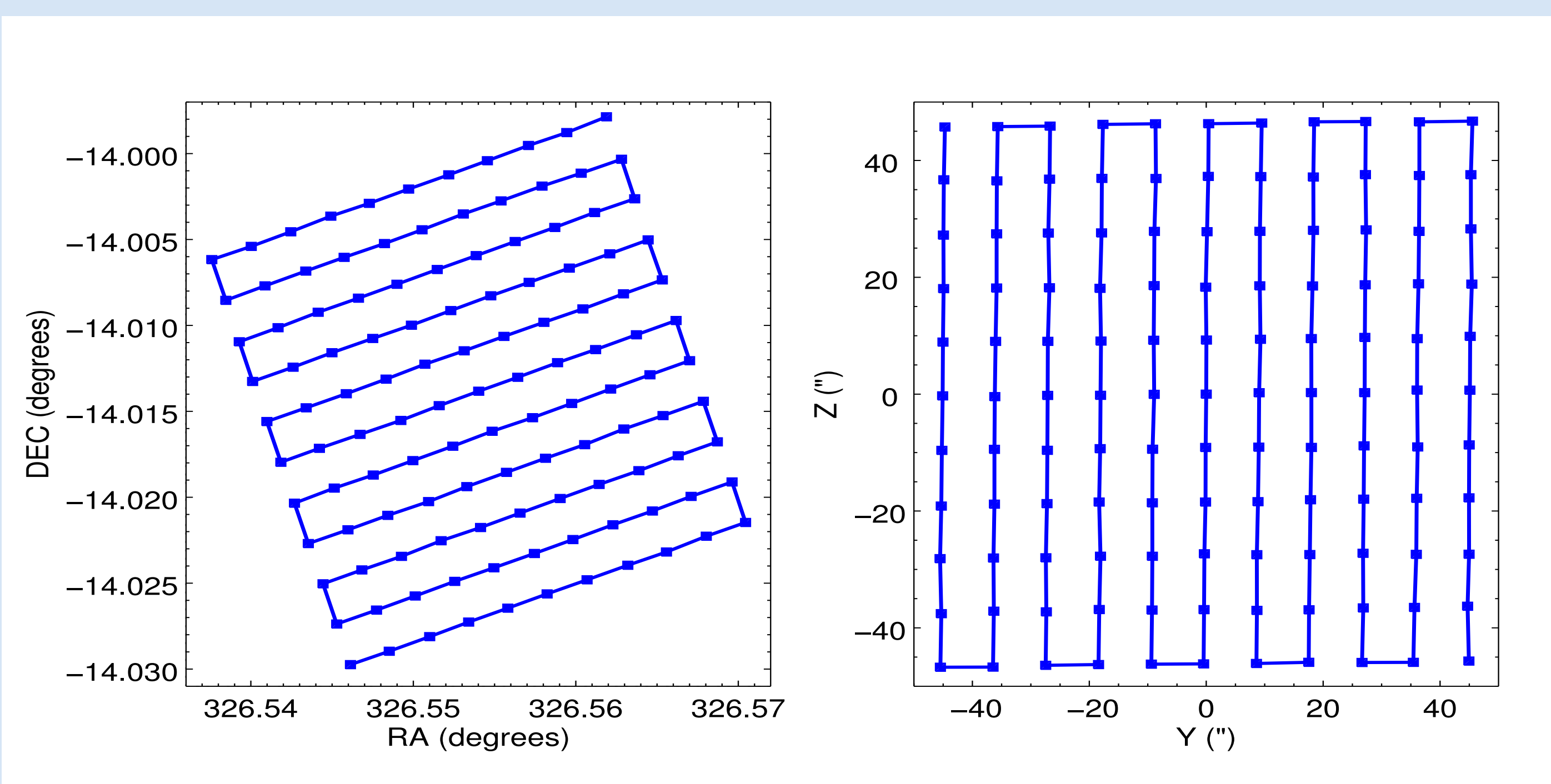


Fig. 1: The raster grid for the Neptune observation on Herschel operational day 210 before (left) and after (right) rotation for alignment with the spacecraft Y and Z axes [3].

Beam decomposition

The SPIRE FTS beam profile was described using,

$$S(r, \lambda) = \sum_{n=0}^{\infty} c_n(\lambda) |\varphi_n(r, \lambda)|^2. \quad (1)$$

where $c_n(\lambda)$ are the wavelength dependent intensity coefficients, r is the radial distance and $\varphi_n(r, \lambda)$ are the radial basis functions of order n .

$$\varphi_n(r, \lambda) = \left(\frac{2}{\pi}\right)^{1/4} \cdot \frac{1}{\sqrt{w_0(\lambda)}} \cdot \frac{1}{\sqrt{2^n \cdot n!}} \cdot H_n\left(\sqrt{2} \frac{r}{w_0(\lambda)}\right) e^{-r^2/w_0^2(\lambda)}. \quad (2)$$

$c_n(\lambda)$ and $w_0(\lambda)$ were determined by fitting.

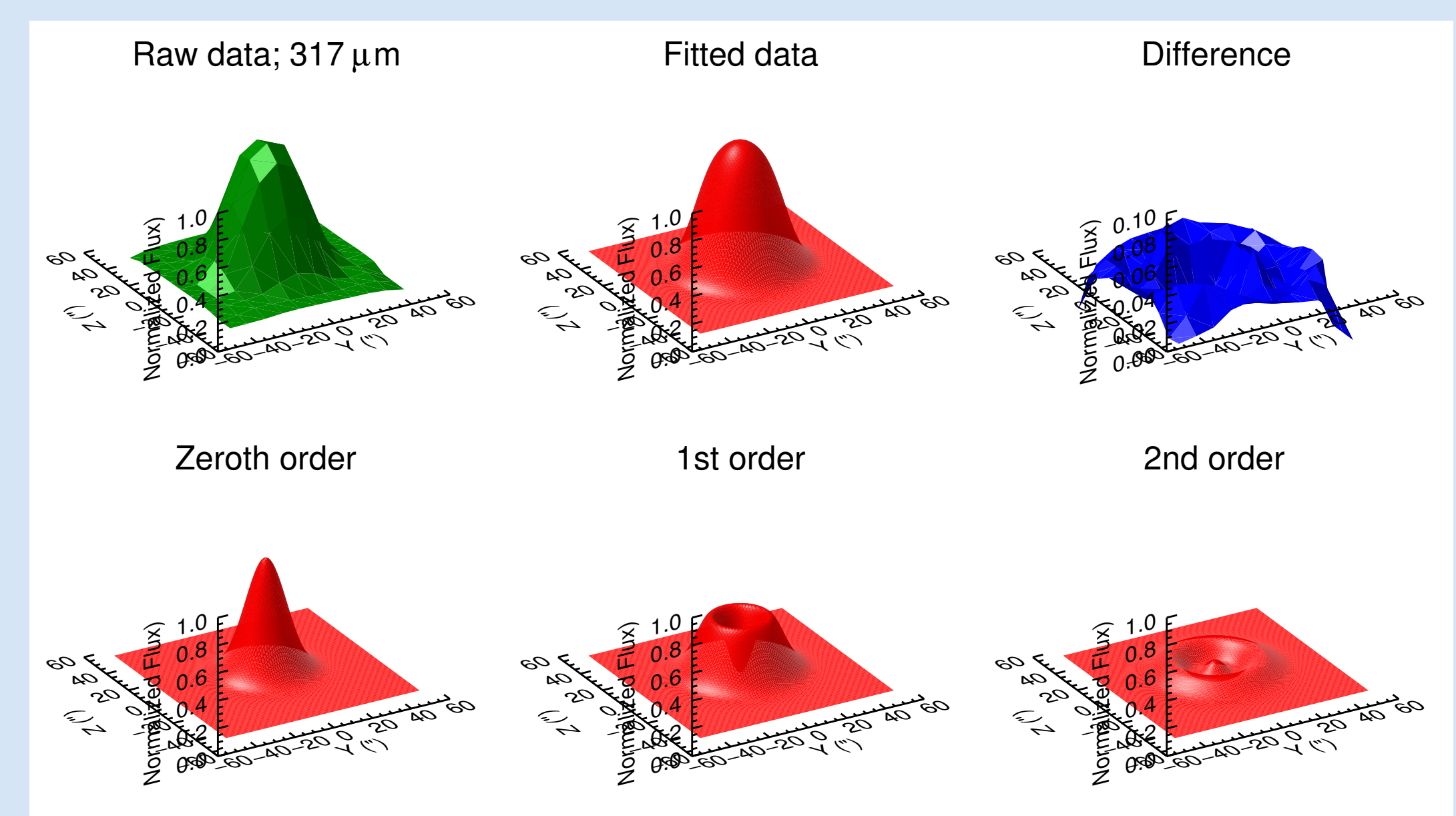


Fig. 2: Surface plots from fitting Neptune data at 317 μm (944 GHz). Bottom row shows a decomposition of the fitted data into the first three orders.

Results and conclusions

Our analysis showed that there is no significant improvement in the residual χ^2 from including terms higher than the zeroth order function (i.e. pure Gaussian) for the SSW band. In contrast, the SLW band is significantly non-Gaussian and required the first three radially symmetric basis functions. The fitted values of $c_n(\lambda)$ and $w_0(\lambda)$ are presented in Makiwa et al. [5].

The FWHM determined from the reconstructed composite beams is shown in Fig. 3(a) for the central detectors and in Fig. 3(b) for selected off-center detectors. In both figures, the FWHM is compared with that expected from diffraction theory.

The longer wavelength end of each SPIRE FTS band agrees well with diffraction theory. This is due to the fact that the beam is expected to be single moded in these regions. The beam shows an increasing deviation from diffraction theory as the number of modes increases.

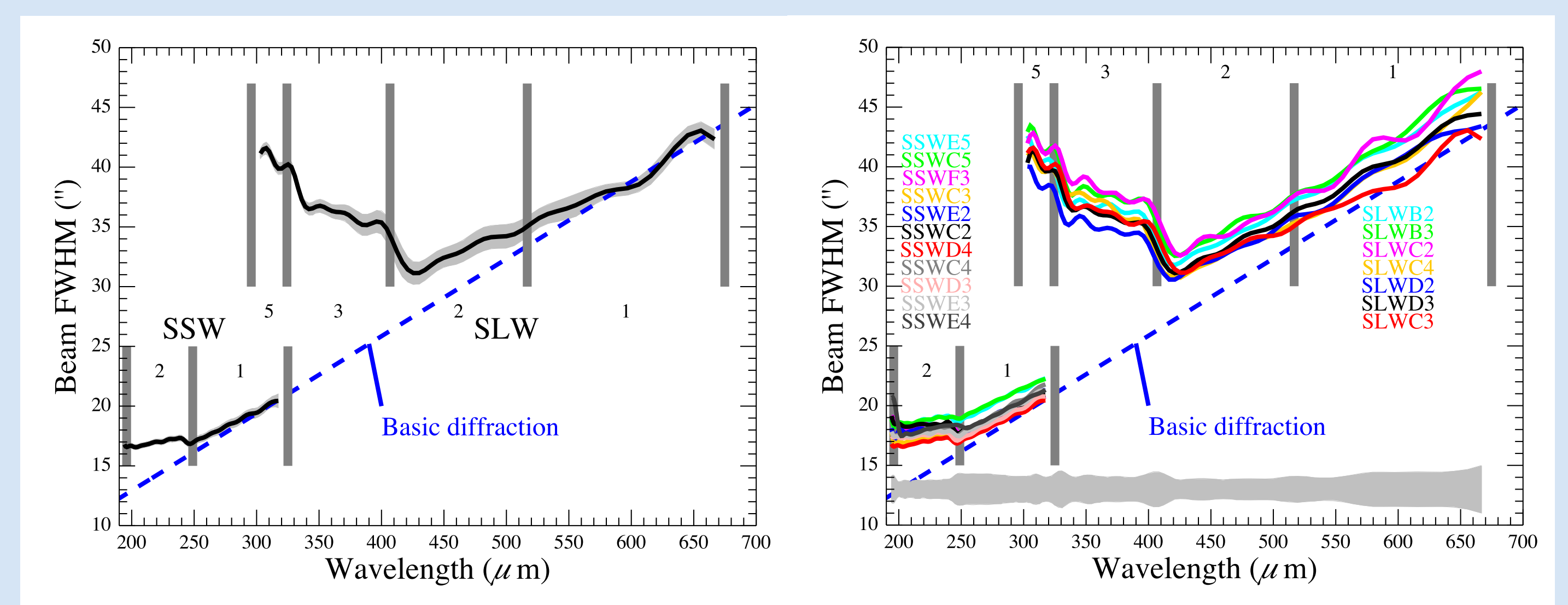


Fig. 3: The measured FWHM of the central detectors (left) and selected off-center detectors (right) compared with diffraction theory. The gray band in the left figure represents the 3σ errors in the measured FWHM while that in the right figure represents the standard deviation. The thick vertical lines indicate the cut-on wavelengths for the different feed-horn modes. The expected number of modes present in these regions are also indicated.

References

- [1] G. L. Pilbratt, J. R. Riedinger, T. Passvogel *et al.*, *A&A*, **518**, L1 (2010). [2] M. J. Griffin *et al.*, *A&A*, **518**, L3, (2010). [3] SPIRE Observer's Manual v2.4. 2011, Herschel Science Centre, HERSCHEL-DOC-0798. [4] S. Ott *et al.*, *ASP Conference Series* **434**, 139-142 (2010). [5] G. Makiwa, *et al.*, Manuscript submitted to *Applied Optics* (2013).